Numerical solution of the Burgers equation with Neumann boundary noise

Bakhtiyar Ghayebi, Seyed Mohammad Hosseini, Dirk Blömker

Numerical Solution of the Burgers equation with Neumann boundary noise

Bakhtiyar Ghayebi[1], S. Mohammad Hosseini[2]

Department of Applied Mathematics, Tarbiat Modares University, P.O. Box 14115-175, Tehran, Iran

Dirk Blömker[3]

Institut für Mathematik, Universität Augsburg, 86159 Augsburg, Germany

Abstract

In this paper we investigate the numerical solution of the one-dimensional Burgers equation with Neumann boundary noise. For the discretization scheme we use the Galerkin approximation in space and the exponential Euler method in time. The impact of the boundary noise on the solution is discussed in several numerical examples. Moreover, we analyze and illustrate some properties of the stochastic term and study the convergence numerically.

Keywords: Burgers equation, Boundary Neumann noise, Galerkin method, Weak approximation, Exponential Euler scheme, impact of noise
2010 MSC: 60H15, 60H35, 65C05, 65C30, 60H10

1. Introduction

Stochastic partial differential equations (SPDE) arise naturally due to environmental fluctuations subject to random influences. Under some physical circumstances the physical boundary of the problem is affected by noise. Such models may be interpreted by partial differential equations (PDEs) with random Neumann boundary conditions [2, 4, 6, 10, 12]. The first paper which studied evolution problems with boundary noise was a paper [20] by Balakrishnan. Later Sowers [10] investigated general reaction diffusion equation with Neumann type boundary noise. Da Prato and Zabczyk [4] discussed the difference between problems with Dirichlet and Neumann boundary noises, as Dirichlet noise does not lead to sufficiently regular solutions. A related work for parabolic problems with boundary noise can be referred to Brzezniak and Peszat [12]. In this paper

---

[1]b.ghayebi@modares.ac.ir & b.ghayebi@qiau.ac.ir
[2]hossei_m@modares.ac.ir
[3]dirk.bloemker@math.uni-augsburg.de

we focus on the following Burgers equation subject to Neumann boundary conditions on the interval $(0, l)$ with boundary noise in only one of the Neumann conditions:

$$\begin{cases} \partial_t u = \nu \partial_{xx} u - u \partial_x u \ , \\ \partial_x u(0,t) = \sigma \dot{\beta}(t) \ , \qquad \partial_x u(l,t) = 0 \ , \\ u(x,0) = u_0(x) \ , \end{cases} \tag{1}$$

Here the scalar $\sigma > 0$ denotes the noise strength and $\{\dot{\beta}(t)\}_{t \geq 0}$ is white noise in time, given by the generalized derivative of a real valued Brownian motion $\{\beta(t)\}_{t \geq 0}$. Finally, the scalar $\nu > 0$ denotes the viscosity. Without loss of generality after rescaling space and time we can assume from now on $\nu = 1$.

For our numerical results we are interested in solutions given in a weak or mild sense. Before we give a definition of these concepts, let us first introduce some basic notation. Fix a terminal time $T > 0$ and let (Ω, F, P) be a probability space, equipped with the filtration $(\mathbb{F}_t)_{t \geq 0}$ induced by the driving Brownian motion.

As candidates for solutions we only consider $L^2(0, l)$-valued stochastic processes $u : \Omega \times [0, T] \to L^2(0, l)$ with continuous paths and adapted to the filtration $(\mathbb{F}_t)_{t \geq 0}$ that satisfy

$$\sup_{t \in [0,T]} \left(\mathrm{E} \, |u(t)|^2_{L^2(0,l)} \right) < \infty \ .$$

According to Da Prato & Zabczyk [4], we consider only solutions u given by the splitting

$$u(x,t) = v(x,t) + w(x,t),$$

where first the process $v(x,t)$ satisfies a linear SPDE (in a weak sense defined later)

$$\begin{cases} \partial_t v = \partial_{xx} v, & 0 < x < l, \quad t > 0, \\ \partial_x v(0,t) = \sigma \dot{\beta}(t), \qquad \partial_x v(l,t) = 0, \\ v(x,0) = 0, \end{cases} \tag{2}$$

and secondly $w(y,t)$ solves the random PDE

$$\begin{cases} \partial_t w = \partial_{xx} w - (v+w)\partial_x(v+w), & 0 < x < l, \quad t > 0, \\ \partial_x w(0,t) = 0, \qquad \partial_x w(l,t) = 0, \\ w(x,0) = u_0(x). \end{cases} \tag{3}$$

We will see later, that the solution of (3) at least locally in time can be obtained by usual deterministic methods based on fixed point theorems. Moreover, it can be well approximated by PDE solvers (see for example [3]). For the linear SPDE we follow [4] and are interested in the solution of the SPDE (2) in the weak sense, given by an Ornstein-Uhlenbeck process called the stochastic convolution. Note that the derivatives of w in general will not exist. Nevertheless, it is well known, that the existence of a sufficiently regular solution to (2) implies the existence of a solution to (3) and thus (1). See for example [4].

2

This paper is organized as follows. In Section 2 we formulate the problem and obtain a series expansion of the solution of (2) given as stochastic convolution. Then we describe the numerical method based on the mild formulation of (2) and (3). In Section 3 we give numerical examples of the Burgers equation subject to random Neumann boundary conditions and study how the noise which is strictly localized on the boundary extends immediately to the entire domain. In Section 4 we compute the difference between solutions with $\sigma = 0$ and $\sigma \neq 0$ using different metrics. In the last section we analyze some properties of the stochastic term and illustrate these properties numerically. Finally, we briefly illustrate the rate of convergence of our numerical scheme by numerical experiments. We think it should also be possible to prove the rate of convergence, but due to non-Lipschitz nonlinearities and poor regularity properties of the stochastic convolution, this would be quite involved.

2. Problem formulation

Denote for the length $l > 0$ of the underlying domain by $L^2(0, l)$ (or short L^2) the standard space of square-integrable functions with the standard scalar product $(u, v)_{L^2} = \int_0^l u(x)v(x)dx$. We also use L^p-spaces $L^p(0, l)$ with norm $\|f\|_{L^p} = (\int_0^l |f(x)|^p dx)^{1/p}$, and similarly L^∞-spaces of measurable and essentially bounded functions.

Definition 2.1. *An $L^2(0, l)$ valued process $(v(t))_{t \in [0,T]}$ with continuous paths and adapted to the filtration $\mathbb{F}$ is a weak solution of (2) if*

$$(v(t), \Psi)_{L^2} = (v_0, \Psi)_{L^2} + \int_0^t (v(s), A\Psi)_{L^2} ds + \beta(t)\Psi(0)$$

for all $t \in [0, T]$ and all smooth test functions $\Psi \in C^\infty([0, l])$ satisfying Neumann boundary conditions

$$\frac{\partial \Psi}{\partial x} = 0 \quad \text{at } x = 0 \text{ and } x = l.$$

Here $A = \partial_{xx}$ is the Laplace operator with the domain of definition $D(A)$, which is given by the subset of the standard Sobolev-space $H^2(0, l)$ of twice weakly differentiable functions with square integrable derivatives satisfying Neumann boundary conditions:

$$D(A) = \left\{ \Psi \in H^2(0, l) : \frac{\partial \Psi}{\partial x}(0) = 0, \frac{\partial \Psi}{\partial x}(l) = 0 \right\}.$$

It is well known (see e.g. [3]) that the operator A has an orthonormal basis of eigenfunctions $\{g_k\}_{k \in \mathbb{N}_0}$ in $L^2(0, l)$ with corresponding non-negative eigenvalues $\{\lambda_k\}_{k \in \mathbb{N}_0}$ of $-A$, where $\mathbb{N}_0$ is the set of all non-negative integers.

To be more precise, in our special problem the eigenfunctions are

$$g_0(x) = \frac{1}{\sqrt{l}}, \qquad g_k(x) = \frac{\sqrt{2}}{\sqrt{l}} \cos\left(\pi k x/l\right), \quad k = 1, 2, \cdots,$$

and the eigenvalues are $\lambda_k = (k\pi/l)^2$, for $k \in \mathbb{N}_0$. Moreover, A generates an analytic semigroup $\{e^{tA}\}_{t\geq 0}$ in L^2 (see [21]). This is defined on the basis by $e^{tA}g_k = e^{-t\lambda_k}g_k$ for all $k \in \mathbb{N}$ and for general L^2-functions by linear extension.

We also define the Sobolev spaces H^α determined for $\alpha > 0$ by the domain of the fractional power $(1 - A)^{\alpha/2}$. In the setting presented here, they can be explicitly defined as

$$H^\alpha = \left\{ \sum_{k=0}^{\infty} u_k g_k \in L^2 \ : \ \|u\|^2_{H^\alpha} = \sum_{k=0}^{\infty}(1 + \lambda_k)^\alpha u_k^2 < \infty \right\}.$$

2.1. Neumann Map

We define the Neumann map $Ɗ : \mathbb{R} \to H^2([0, l])$, which is a continuous linear operator between these spaces (see [11]). For any $\gamma \in \mathbb{R}$ the operator $Ɗ$ is defined by the solution of the following Neumann problem

$$(1 - A)\,Ɗ\gamma = 0, \qquad \partial_x Ɗ\gamma(0) = \gamma, \qquad \partial_x Ɗ\gamma(l) = 0 \ .$$

In fact, there is an explicit expression for this linear operator

$$Ɗ(\gamma)[x] = \frac{e^x + e^{2l}e^{-x}}{1 - e^{2l}}\gamma.$$

From [5] we immediately obtain the following theorem about the weak solution of (2) in the Sobolev space H^α, $\alpha < 1/2$. Later we will see that solutions fail to be in L^∞, in contrast to the usual regularity results for stochastic convolutions with additive noise.

Theorem 2.2. *For the Neumann boundary value problem (2) there is a unique weak solution, which is in the space H^α for all $\alpha < \frac{1}{2}$. Moreover, the solution is given by the mild formulation as a stochastic convolution*

$$v(t) = (1 - A) \int_0^t e^{A(t-s)}Ɗ\sigma d\beta(s).$$

For the proof, we just remark that the uniqueness follows directly from the definition and Gronwall's Lemma. For the regularity in H^α one can use the series expansion derived below in (4) and the series expansion of the H^α-spaces.

Let us now follow [6] to provide an explicit formula for v in terms of Fourier series. For $\gamma \in \mathbb{R}$, by the definition of $Ɗ$ and using integration by parts we obtain for $g \in D(A)$

$$(Ɗ\gamma, (1 - A)g)_{L^2} = (Ɗ\gamma, g)_{L^2} - \int_0^l Ɗ\gamma \cdot g_{xx}dx$$

$$= (Ɗ\gamma, g)_{L^2} - \int_0^l (Ɗ\gamma)_{xx}gdx + (Ɗ\gamma)_x \cdot g\big|_0^l$$

$$= -\gamma g(0).$$

4

Hence,

$$(v(t), g_k)_{L^2} = \left(\int_0^t e^{A(t-s)} \mathrm{D}\sigma d\beta(s), (1-A) g_k \right)_{L^2}$$

$$= \int_0^t e^{-(t-s)\lambda_k} (\mathrm{D}\sigma d\beta(s), (1-A) g_k)_{L^2}$$

$$= \sigma g_k(0) \int_0^t e^{-(t-s)\lambda_k} d\beta(s).$$

Therefore, we obtain

$$v(t) = \sigma \sum_{k \in \mathbb{N}_0} g_k(0) \int_0^t e^{-(t-s)\lambda_k} d\beta(s) g_k.$$

Finally, we have

$$v(t) = \sigma g_1(0) \sum_{k \in \mathbb{N}} \int_0^t e^{-(t-s)\lambda_k} d\beta(s) g_k + \sigma g_0^2(0)\beta(t). \tag{4}$$

This looks very similar to a standard stochastic convolution with space-time white noise, but the key difference is that all Brownian motions in the series are actually the same. We would obtain exactly the same stochastic convolution, in case of an additive point forcing of the type $\delta_0 d\beta$, where δ_0 is the Dirac-function on the left boundary $x = 0$.

2.1.1. The effect of Noise On Both Sides

Let us briefly remark on the effect of noise in both boundary conditions. We now consider (1) with the new conditions $\partial_x u(0,t) = \sigma_1 \dot{\beta}_1(t), \partial_x u(l,t) = \sigma_2 \dot{\beta}_2(t)$. In that case we can define the Neumann map $\hat{\mathrm{D}} : \mathbb{R}^2 \to H^2(0,l)$ for any $\gamma = (\gamma_1, \gamma_2) \in \mathbb{R}^2$ by the solution of

$$(1-A)\hat{\mathrm{D}}\gamma = 0, \qquad \partial_x \hat{\mathrm{D}}\gamma_1(0) = \gamma_1, \qquad \partial_x \mathrm{D}\gamma_2(l) = \gamma_2 \ .$$

Furthermore, also in this case we have an explicit expression for this linear operator given by

$$\hat{\mathrm{D}}(\gamma)[x] = \frac{e^x + e^{2l}e^{-x}}{1 - e^{2l}}\gamma_1 + \frac{e^x + e^{-x}}{e^l - e^{-l}}\gamma_2.$$

Then with a similar proof as before we obtain the mild solution *v(t)* of the linear SPDE for these two-sided random Neumann conditions as follows:

$$v(t) = \sigma_1 g_1(0) \sum_{k \in \mathbb{N}} \int_0^t e^{-(t-s)\lambda_k} d\beta_1(s) g_k + \sigma g_0^2(0)\beta_1(t)$$

$$+ \sigma_2 \sum_{k \in \mathbb{N}} (-1)^k g_k(1) \int_0^t e^{-(t-s)\lambda_k} d\beta_2(s) g_k + \sigma_2 g_0^2(1)\beta_2(t). \tag{5}$$

5

Note that we can again easily check that $\mathbb{E}\|v(t)\|_{H^\alpha}^2 < \infty$, if and only if $\sum_{k=0}^\infty \lambda_k^{1-\alpha} < \infty$, which in turn is true, if and only if $\alpha < \frac{1}{2}$.

The structure of the noise influence is very similar, and therefore in the sequel for simplicity we will only consider (1) with noise only in one of the boundary conditions.

2.2. Mild Formulation

Now we turn to the non-linear equation. The mild solution of the random PDE (3) is given by the solution of the following fixed point equation

$$w(t) = e^{tA}u_0 + \int_0^t e^{A(t-s)}\Big(-\frac{1}{2}\frac{\partial}{\partial x}\left(v(s) + w(s)\right)^2 \Big)ds, \qquad \text{for } t > 0.$$

By the substitution $u = w + v$, this is equivalent to the mild solution of (1) (see Theorem 2.3), which is given as a solution of

$$u(t) = e^{tA}u_0 + \int_0^t e^{A(t-s)}\Big(-\frac{1}{2}\frac{\partial}{\partial x}u^2(s)\Big)ds + v(t).$$

The main advantage is that for any realization of v one can obtain path-wise the uniquely defined solution u by standard deterministic fixed point arguments.

Theorem 2.3. *Suppose for the Ornstein-Uhlenbeck processes $v \in C^0([0,T], L^2)$, and define $F(u) = -\frac{1}{2}\frac{\partial}{\partial x}u^2$. Then for every initial condition $u_0 \in L^2$ there exists $u \in C^0([0,T], L^2)$ which satisfies for all $t \in [0,T]$*

$$u(t) = e^{tA}u_0 + \int_0^t e^{A(t-s)}F(u(s))ds + v(t).$$

Sketch of Proof. See for example chapter 15 of [2], or the standard PDE reference [24]. It is sufficient to verify that F is a locally Lipschitz continuous mapping from L^2 to $H^{-\alpha}$ for some $\alpha \in (3/2, 2)$. Then the claim for local solution follows by Banach's fixed point theorem.

Moreover, one can use the fact that $w = u - v$ satisfies the random PDE

$$\partial_t w = Aw + F(w + v)$$

where standard a-priori type estimates for the L^2-norm of w show that the solution w exists up to time T. □

2.3. Numerical scheme

For simplicity of presentation suppose in the following that the length of the interval is given by $l = 1$. Nevertheless, this is not a severe restriction, as we can rescale the domain by a factor $1/l$, and time by $1/l^2$, which just results in a small ν and a changed noise strength.

Similar as the numerical scheme in [23], which is based on the work of Jentzen and Kloeden [7, 8] we consider the exponential Euler method for the Galerkin

approximation of the mild solution of the Burgers equation (1). Nevertheless, one might discuss whether this scheme is still efficient in our case, because the random numbers that need to be generated are highly correlated, but we do not discuss this here.

Recall the mild formulation

$$u(t) = e^{tA}u(0) + \int_0^t e^{A(t-s)}F(u(s))ds + (1-A)\int_0^t e^{A(t-s)}D\sigma d\beta(s) , \qquad (6)$$

where we have defined the nonlinearity

$$F(u) = -\frac{1}{2}\frac{\partial}{\partial x}(u^2) .$$

Projecting equation (6) onto the subspace

$$X_N = \text{span}\{g_0, g_1, ..., g_N\},$$

of $L^2(0, l)$, spanned by the first $N+1$ eigenfunctions $g_0, g_1, ..., g_N$, the Galerkin approximation with $N+1$ degrees of freedom in $L^2(0, 1)$ is given by

$$u^N(t) = \sum_{n=0}^N u_n(t)g_n .$$

Additionally, for the nonlinearity we approximate

$$F^{(N)}(u^N(t)) = \sum_{n=0}^N F_n(u^N(t))g_n.$$

Here we used the definitions

$$u_n(t) = (u^N(t), g_n)_{L^2}, \qquad F_n(u^N) = (F(u^N), g_n)_{L^2}, \qquad n = 0, 1, ..., N.$$

Note that both u_n and F_n depend on N, but we suppress this dependence in the notation.

From Equations (6) and (4), we obtain the Galerkin approximation in terms of the following stochastic differential equation (SDE) in $\mathbb{R}^{N+1}$ of the form,

$$u_n(t) = e^{-t\lambda_n}u_n(0) + \int_0^t e^{-\lambda_n(t-s)}F_n(u^N(s))ds + \sigma g_n(0)\int_0^t e^{-(t-s)\lambda_n}d\beta(s) .$$
$$(7)$$

Thus for a fixed small time $\Delta t > 0$ we obtain

$$u_n(t + \Delta t) = e^{-\Delta t\lambda_n}u_n(t) + \int_0^{\Delta t} e^{-\lambda_n(\Delta t-s)}F_n(u^N(t+s))ds$$

$$+ \sigma g_n(0)\int_0^{\Delta t} e^{-(\Delta t-s)\lambda_n}d\beta(t+s) .$$

7

First we rewrite the stochastic integrals in the last line, which is a Gaussian, by the square root of the variance times a standard Gaussian, which we denote by R_n. Obviously, R_n depends on $\beta(s)$ for $s \in [t, t + \Delta t]$ and on the scalars t, λ_n, σ and Δt. To be more precise, we define R_n for $n \in \mathbb{N}$ by the equality

$$\left(\frac{1}{\lambda_n}\left(1 - e^{-2\lambda_n \Delta t}\right)\right)^{\frac{1}{2}} \sigma R_n = \sigma g_n(0) \int_0^{\Delta t} e^{-(\Delta t - s)\lambda_n} d\beta(t + s)$$

and for $n = 0$ by

$$\sqrt{\Delta t} \sigma R_0 = \sigma g_0(0)[\beta(t + \Delta t) - \beta(t)] .$$

To solve the nonlinear equation, we apply an exponential Euler-scheme. This yields

$$u_n(t + \Delta t) \approx e^{-\lambda_n \Delta t} u_n(t) + \frac{1 - e^{-\lambda_n \Delta t}}{\lambda_n} F_n(u^N(t)) + \left(\frac{1}{\lambda_n}\left(1 - e^{-2\lambda_n \Delta t}\right)\right)^{\frac{1}{2}} \sigma R_n$$

$$(8)$$

for $n = 1, 2, ..., N$, and for $n = 0$

$$u_0(t + \Delta t) = u_0(t) + F_0(u^N(t))\Delta t + \sqrt{\Delta t} \sigma R_0, \qquad (9)$$

where we again stress that the normal random variables R_n depend all on the same Brownian motion. Finally, we can define the full numerical scheme

$$u_{n,k+1} = e^{-\lambda_n \Delta t} u_{n,k} + \frac{1 - e^{-\lambda_n \Delta t}}{\lambda_n} F_n(u_k^N) + \left(\frac{1}{\lambda_n}\left(1 - e^{-2\lambda_n \Delta t}\right)\right)^{\frac{1}{2}} \sigma R_{n,k} \quad (10)$$

for $n = 1, 2, ..., N$, and

$$u_{0,k+1} = u_{0,k} + F_0(u_k^N)\Delta t + \sqrt{\Delta t} \sigma R_{0,k} \qquad (11)$$

where for fixed n the family $\{R_{n,k}\}_{k=0,1,...}$ consists of independent standard normally distributed random variables, which are nevertheless highly correlated when n is varied. In the next section we discuss in more detail how these random numbers can be generated efficiently. Once we calculated all u_n, we obtain the approximate solution

$$u^N(x, t) = \sum_{n=0}^{N} u_n(t) g_n(x).$$

Note that here we extend by linear interpolation the real-valued processes u_n, which are only defined on discrete time-points.

3. Numerical simulations

In this section as an example we fix the initial condition $u_0(x) = \frac{6}{5}\cos(\pi x)$ and rely on the numerical method presented in (9) and (10) to solve the problem
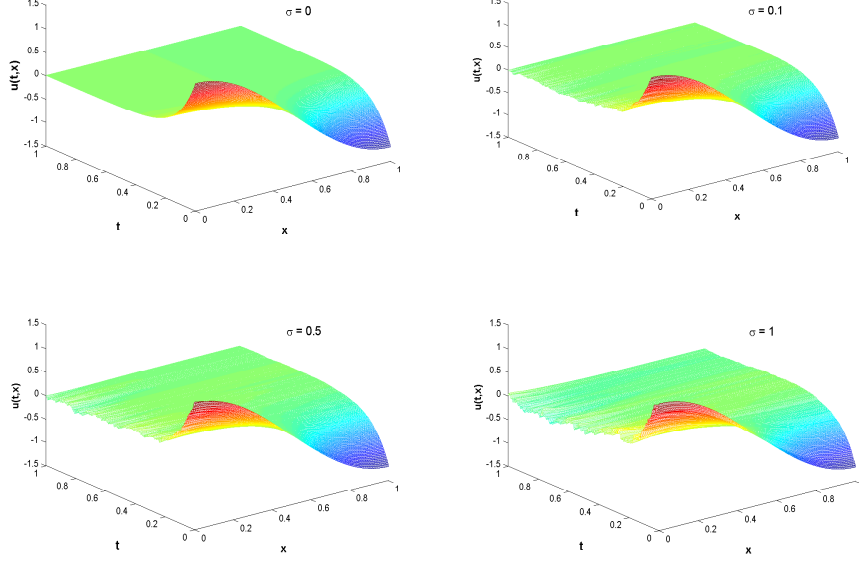
Figure 1: Solution of Burgers equation with Neumann boundary noise, for noise intensities: $\sigma = 0,\ 0.1,\ 0.5,\ 1$ and with $u_0(x) = \frac{6}{5}\cos(\pi x), N = 200, \Delta t = 1/300, \nu = 1$.

(1). See Figures 1 and 2 for snapshots of solutions. There is nothing special about the initial condition and other choices would yield similar results.

Note that the Gaussian random variables $R_{n,k}$ are highly dependent on each other for fixed k, and we need to take this into account in the numerical simulation. We briefly sketch how this is done in the simulation. Consider for fixed $t \geq 0$ the standard Brownian motion $\beta^{(t)}$ defined by $\beta^{(t)}(s) = \beta(t+s) - \beta(t)$. We define the real-valued Gaussians

$$X_n = \int_0^{\Delta t} e^{-(\Delta t - s)\lambda_n} d\beta^{(t)}(s) = \left(\frac{1}{2\lambda_n} \left(1 - e^{-2\lambda_n \Delta t} \right) \right)^{\frac{1}{2}} R_n \ .$$

Then by direct calculation, we obtain

$$\mathbb{E} X_n X_m = \int_0^{\Delta t} e^{-(\Delta t - s)\lambda_n} e^{-(\Delta t - s)\lambda_m} ds = \frac{1}{\lambda_n + \lambda_m}(1 - e^{-\Delta t(\lambda_n + \lambda_m)}) \neq 0.$$

Therefore, for generating X_n and thus the R_n, let Σ be the covariance matrix of X, which is an $n \times n$ matrix where the $(i,j)^{th}$ element is given by $\Sigma_{i,j} := Cov(X_i, X_j)$. Our aim at this step is to generate the Gaussian vector $X = (X_1, X_2, ..., X_n) \sim \texttt{MN}(0,\Sigma)$. Here $\texttt{MN}(0,\Sigma)$ denotes a vector valued Gaussian with mean 0 and covariance operator Σ.

Let us recall that for i.i.d. standard Gaussians $Z_i \sim \texttt{N}(0,1)$ for $i = 1, 2, ..., n$,

we obtain:

$$l_1 Z_1 + l_2 Z_2 + ... + l_n Z_n \sim \mathtt{N}(0, \sigma^2)$$

where $\sigma^2 := l_1^2 + l_2^2 + ... l_n^2$. That is, a linear combination of independent normal random variables is again normal.

More generally, let L be an $n \times m$ matrix and let $\mathbf{Z} = (Z_1, Z_2, ..., Z_n) \sim \mathtt{MN}(0, I_n)$ where I_n is the $n \times n$ identity matrix, then $L^T \mathbf{Z} \sim \mathtt{MN}(0, L^T L)$. Hence, our problem clearly reduces to finding L such that $L^T L = \Sigma$. We can find such a matrix, L, using the Cholesky decomposition of Σ.

Hence, we can now generate for any k the Gaussians $R_{n,k}$, and with these random numbers we can apply our numerical method to the problem (1) with $u_0(x) = \frac{6}{5} \cos(\pi x)$. Note that for comparing the solutions with different N pathwise, we first calculate the random variables X_i for some very large N and then use them for all simulations with smaller N.

The results for $\nu = 1$ and various noise intensities σ are shown in Figure 1. As the noise intensity σ grows, the corresponding solution undulates more and more and spreads all over the domain.

Small ν means after rescaling that we study large domains and slow times with $\nu = 1$. So for another illustration of the impact of noise, we also increase the noise level by adding a small constant $\nu = 1/50$ in front of the u_{xx} in (1), see Figure 2. This figure confirms that by increasing the effect of noise the solution goes to 0 much slower. Further investigation on the impact of the noise on the solution is carried out in the following Section.

4. The impact of boundary noise on the solution

In order to quantify the impact of the noise on the solution of the Burgers equation with Neumann boundary conditions, we compute the difference between solutions corresponding to $\sigma = 0$ and $\sigma \neq 0$ using different metrics [10, 13].

To observe better the impact of noise by increasing the amount of noise, we restrict ourselves to the case of initial condition $u_0(x) = 0$. In that case obviously the deterministic solution corresponding to $\sigma = 0$ is identically 0 for all times.

We then compute the root mean square difference (RMSD) between the numerical solutions of equation without noise ($\sigma = 0$) and with the Neumann boundary noise ($\sigma \neq 0$). Similar as in [22], we use the following three metrics. Recall that $u_{\sigma=0}(x, t) = 0$, as we have chosen here $u(0) = 0$.

Definition 4.1. *We define*

1. $RMSD_1(x, t) = \sqrt{\mathrm{E}|u_{\sigma \neq 0}(x, t) - u_{\sigma=0}(x, t)|^2}$

2. $RMSD_2(x) = \sqrt{\mathrm{E} \int_0^1 |u_{\sigma \neq 0}(x, t) - u_{\sigma=0}(x, t)|^2 dt}$

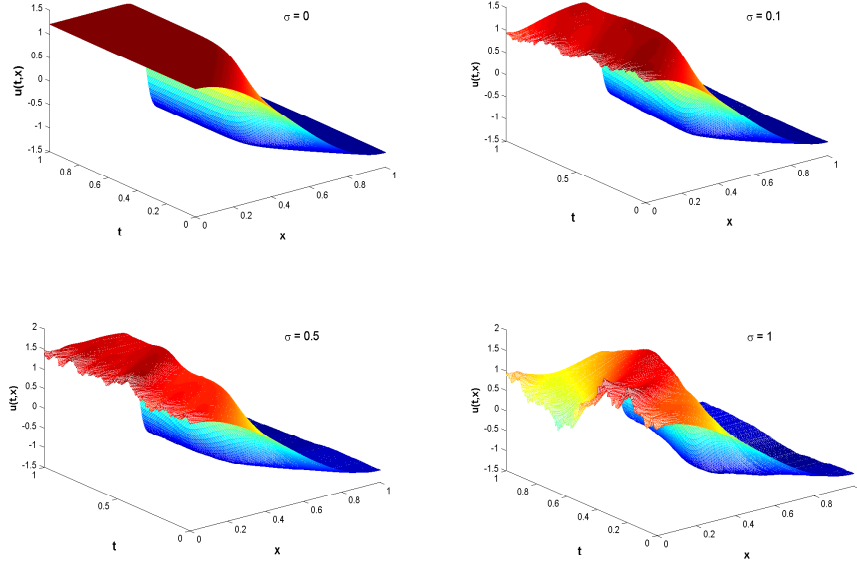3. $RMSD_3(t) = \sqrt{\mathrm{E} \int_0^1 |u_{\sigma \neq 0}(x, t) - u_{\sigma=0}(x, t)|^2 dx}$

Figure 2: Solution of Burgers equation with Neumann boundary noise, for noise intensities: $\sigma = 0, \ 0.1, \ 0.5, \ 1$ and with $u_0(x) = \frac{6}{5}\cos(\pi x), N = 200, \Delta t = 1/300, \nu = 1/50$. Recall that small ν corresponds to slow time and large domains. The noise has significantly less impact at $x = 1$.

The plots in Figure 3 illustrate the impact of increasing noise very clearly, showing that the noise on the boundary grows immediately into the entire domain. Moreover, its impact at $x = 1$ is not negligible. For this result 30 realizations have been used to roughly calculate the mean. Also, see Figures 4-6, it is observed that with $\sigma = 0.01$ the noise on the boundary $x = 0$ spreads at once to the interior domain $(0 < x < 1)$. In addition, in Figure 7 we sketch

$$\sqrt{\mathrm{E}\left|u_{\sigma \neq 0}(x,t) - \int_0^1 u_{\sigma \neq 0}(x,t)dx\right|^2} \quad \text{for } \sigma = 0.01.$$

In comparison with Figure 3 the the impact of the noise on the other non-constant modes is significantly smaller, but still the noise spreads immediately through the whole domain. The main impact on the noise at $x = 1$ seems to be by the constant mode, but also the other modes are not negligible.
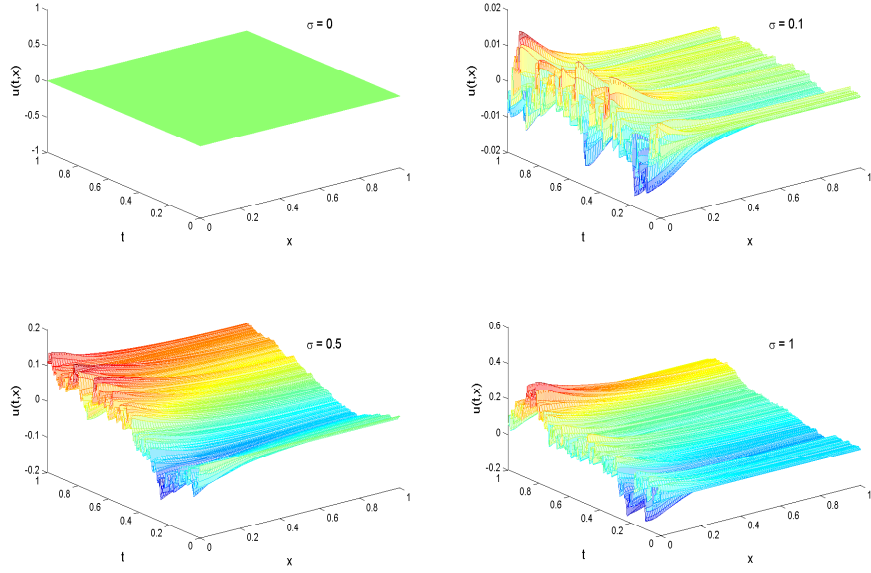
Figure 3: Solution of Burgers equation with Neumann boundary noise, for noise intensities: $\sigma = 0,\ 0.1,\ 0.5,\ 1$ and with $u_0(x) = 0$, $N = 200$, $\Delta t = 1/300$, $\nu = 1$. The noise spreads immediately through the whole domain, but it seems that the main impact is on the constant Fourier-mode.
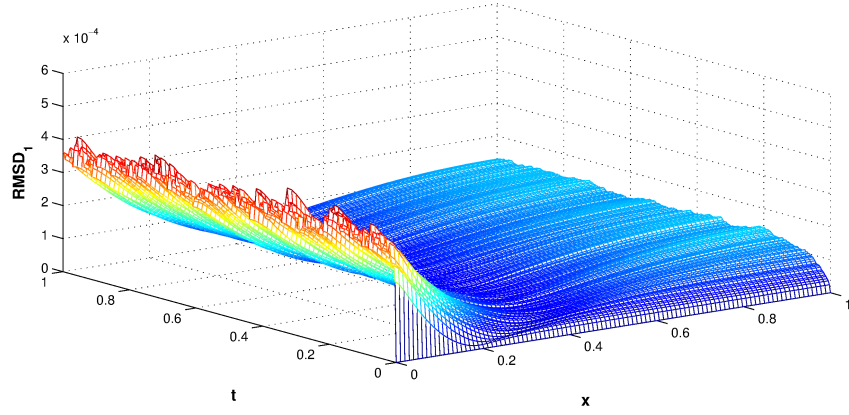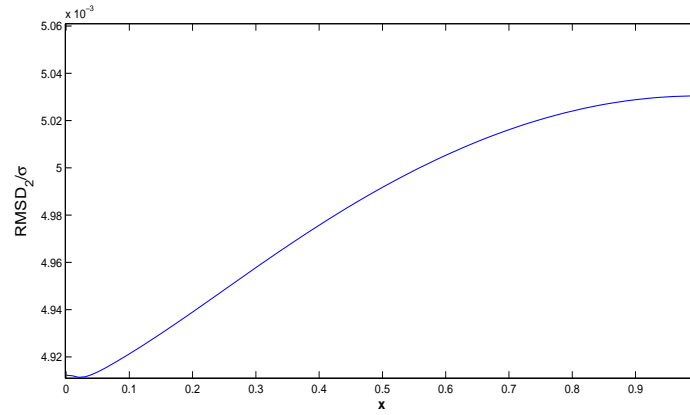

Figure 4: Root mean square difference $(RMSD_1)$ of the Burgers equation with random Neumann boundary noise, with respect to time and space, for $\sigma = 0.01$, with $u_0(x) = 0$.

12

Figure 5: Root mean square difference $(RMSD_2)/\sigma$ of the Burgers equation with random Neumann boundary noise, with respect to space, for $\sigma = 0.01$, with $u_0(x) = 0$. The impact of noise decays from the noise source $x = 0$ to $x = 1$. Although the order of the impact at both sides is comparable.
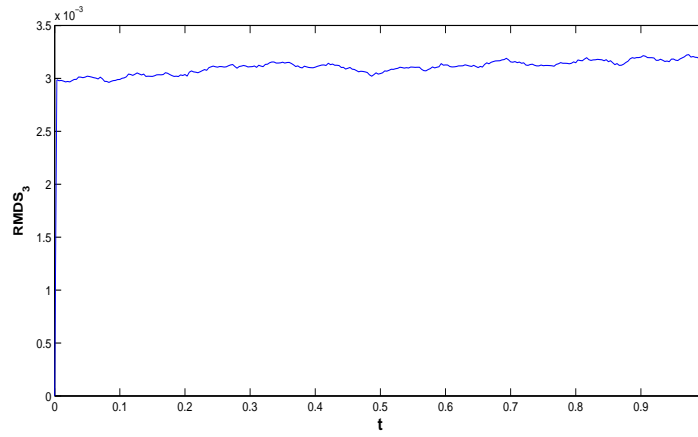

Figure 6: Root mean square difference $(RMSD_3)$ of the Burgers equation with random Neumann boundary noise, with respect to time, for $\sigma = 0.01$. and $u_0(x) = 0$. At each point of time the average impact of noise is roughly the same, as expected.
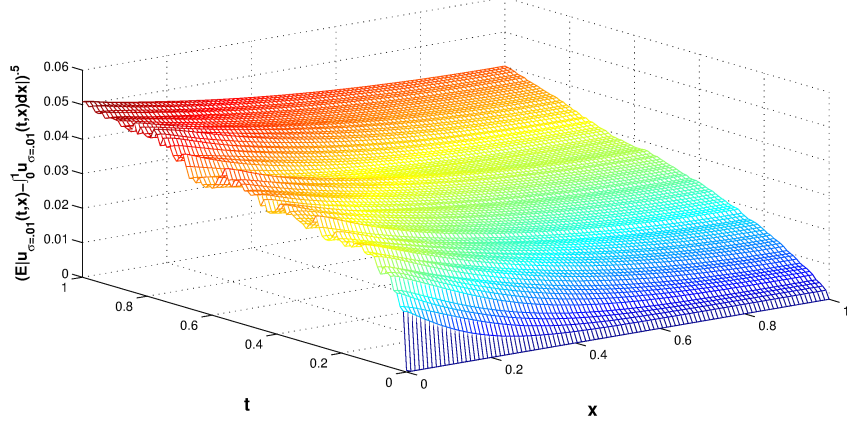
13

Figure 7: $\sqrt{\mathrm{E}\left|u_{\sigma\neq 0}(x,t) - \int_0^1 u_{\sigma\neq 0}(x,t)dx\right|^2}$ of the Burgers equation with random Neumann boundary noise, with respect to time and space, for $\sigma = 0.01$, with $u_0(x) = 0$.

5. Analysis of $v(\mathbf{t})$

In this section firstly we calculate $\mathrm{E}|v(t,x)|^2$ and then show that $v(t,0)$ is unbounded. This shows that numerical analysis in L^∞-norm is not possible. For this from (4) we have

$$
\mathrm{E}|v(t,x)|^2 = \mathrm{E}\left(\sigma g_1(0)\sum_{k=1}^{\infty}\int_0^t e^{-(t-s)\lambda_k}d\beta_s g_k(x) + \sigma g_0^2(0)\beta(t)\right)^2
$$

$$
= \mathrm{E}\Bigg(\left(\sigma g_1(0)\sum_{k=1}^{\infty}\int_0^t e^{-(t-s)\lambda_k}d\beta_s g_k(x)\right)^2
$$

$$
+ 2\sigma^2 g_1(0)g_0^2(0)\beta(t)\sum_{k=1}^{\infty}\int_0^t e^{-(t-s)\lambda_k}d\beta_s g_k(x) + \left(\sigma g_0^2(0)\beta(t)\right)^2\Bigg)
$$

$$
\tag{12}
$$

$$
= \mathrm{E}\left(\sigma g_1(0)\sum_{k=1}^{\infty}\int_0^t e^{-(t-s)\lambda_k}d\beta_s g_k(x)\right)^2
$$

$$
+ \mathrm{E}\left(2\sigma^2 g_1^3(0)\beta(t)\sum_{k=1}^{\infty}\int_0^t e^{-(t-s)\lambda_k}d\beta_s g_k(x)\right) + \mathrm{E}\left(\sigma g_0^2(0)\beta(t)\right)^2
$$

14

Using the Itô isometry we obtain

$$
\begin{aligned}
\mathrm{E}|v(t,x)|^2 &= \sigma^2 g_1^2(0) \sum_{k=1}^{\infty} \sum_{l=1}^{\infty} \frac{\left(1 - e^{-t(\lambda_k + \lambda_l)}\right) g_k(x) g_l(x)}{\lambda_k + \lambda_l} \\
&\quad + 2\sigma^2 g_1(0) g_0^2(0) \sum_{k=1}^{\infty} \frac{\left(1 - e^{-t\lambda_k}\right) g_k(x)}{\lambda_k} + \sigma^2 g_0^4(0) t .
\end{aligned}
\tag{13}
$$

Now we plug in the precise values for the λ_k and g_k and derive

$$
\begin{aligned}
\mathrm{E}|v(t,x)|^2 &= \frac{2\sigma^2}{\pi^2} \sum_{k=1}^{\infty} \sum_{l=1}^{\infty} \frac{\left(1 - e^{-t\pi^2(k^2 + l^2)}\right) \cos(kx) \cos(lx)}{k^2 + l^2} \\
&\quad + \frac{2\sqrt{2}\sigma^2}{\pi^2} \sum_{k=1}^{\infty} \frac{\left(1 - e^{-t\pi^2 k^2}\right) \cos(kx)}{k^2} + \sigma^2 t.
\end{aligned}
\tag{14}
$$

Now let $x = 0$ in (12). Then,

$$
\mathrm{E}|v(t,0)|^2 = \mathrm{E}\left| \int_0^t \left(\sigma g_1(0) \sum_{k=1}^{\infty} e^{-\pi^2(t-s)k^2} g_k(0) + \sigma g_0^2(0) \right) d\beta_s \right|^2 .
\tag{15}
$$

From Itô isometry we obtain

$$
\begin{aligned}
\mathrm{E}|v(t,0)|^2 &= \int_0^t \left(\sigma g_1(0) \sum_{k=1}^{\infty} e^{-\pi^2(t-s)k^2} g_k(0) + \sigma g_0^2(0) \right)^2 ds \\
&\geq C \int_0^t \left(\int_1^{\infty} e^{-\pi^2(t-s)x^2} dx \right)^2 ds
\end{aligned}
$$

where C depends on σ and $g_k(0)$. Now let $I = \int_1^{\infty} e^{-\pi^2(t-s)x^2} dx = \int_1^{\infty} e^{-\pi^2(t-s)y^2} dy$. Then we have

$$
I^2 = \int_1^{\infty} \int_1^{\infty} e^{-\pi^2(t-s)(x^2 + y^2)} dx\, dy.
$$

This is bounded from below by an integral over the smaller set given by $(x,y) \in [0,\infty)^2$ where $x^2 + y^2 > 2$. Or in terms of polar coordinates $r > \sqrt{2}$ and angle $\theta \in [0, \pi/2]$.

Using the transformation via polar coordinates yields

$$
I^2 \geq \int_0^{\frac{\pi}{2}} \int_{\sqrt{2}}^{\infty} e^{-\pi^2(t-s)r^2} r\, dr\, d\theta = \frac{e^{-2\pi^2(t-s)}}{2\pi^2(t-s)}.
$$

Therefore,

$$
\mathrm{E}|v(t,0)|^2 \geq C \int_0^t \frac{e^{-2\pi^2(t-s)}}{2\pi^2(t-s)} ds = C \frac{1}{2\pi^2} \int_0^t \frac{e^{-2\pi^2 s}}{s} ds = \infty
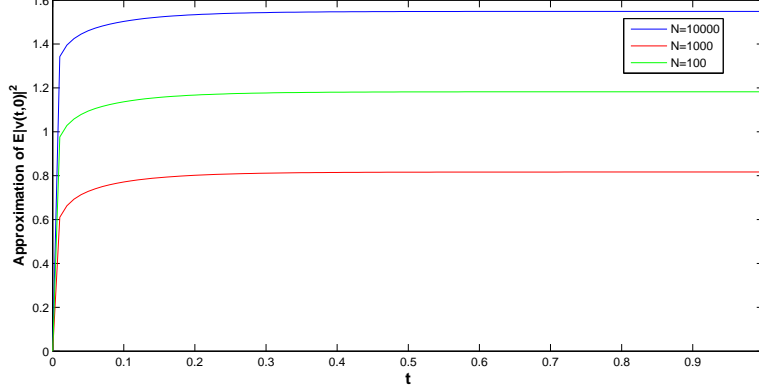$$

15

Figure 8: Approximation of $\mathrm{E}|v(t,0)|^2$ with respect to time, sum of first N terms of right-hand of (14) for $N = 100, 1000$, and 10000, confirming unboundedness of $\mathrm{E}|v(t,0)|^2$. We see a logarithmic divergence as we would expect.

and hence $\mathrm{E}|v(t,0)|^2 = \infty$. Therefore, we have shown that the stochastic convolution v is not bounded at 0. Because of this lack of regularity we can not expect uniform bounds on the solution.

For more illustrative properties we plotted the approximation of $\mathrm{E}|v(t,x)|^2$ for $x = 0$, $x = 0.1$ and $x = 1$ in Figure 8, according to Figure 8 we see that $\mathrm{E}|v(t,0)|^2$ is divergent and $\mathrm{E}|v(t,x)|^2$ for $x \neq 0$ is convergent, see Figure 9. The divergence is logarithmic, as expected.

In addition we plotted in Figures 10-12 the Monte-Carlo approximation of $\mathrm{E}|v(t,x)|^2$ with respect to time and $x = 1$ from (14) and also $\mathrm{E}|u(t,x)|^2$ for $N = 200$ and 300, in which only 50 realizations have been used to calculate the mean. Even with a few modes and very few realizations, the divergence is already obvious although very slow.

In order to understand more about the properties of the stochastic process $v(t)$, in the lines of [6], we compare $v(t)$ to another stochastic convolution derived by an equation with additive noise given by a cylindrical Wiener process

$$W(t) = \sum_{k=1}^{\infty} \beta_k(t) g_k + \beta_0 \ ,$$

where the family $\{\beta_k\}_{k \in \mathbb{N}_0}$ consists of i.i.d. standard Brownian motions. The Wiener process drives the SPDE in (17) as additive noise and not via Neumann noise. Thus we consider for noise strength α defined later

$$\mathrm{Z}(t) = \alpha \sum_{k \in \mathbb{N}} \int_0^t e^{-(t-s)\lambda_k} d\beta_k(s) g_k + \alpha \beta_0(t). \tag{16}$$
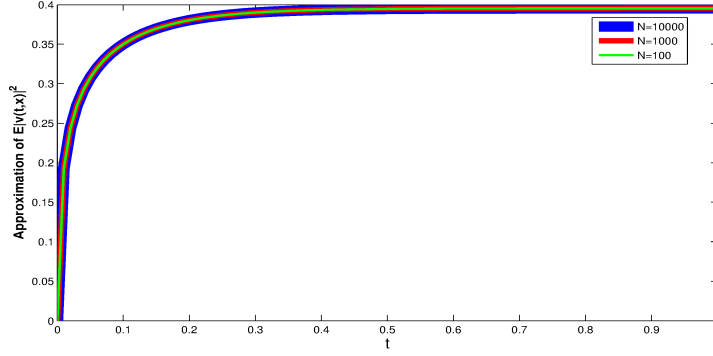
16

Figure 9: Approximation of $\mathrm{E}|v(t,x)|^2$ with respect to time and $x = .1$, sum of first N terms of right-hand of (14) for $N = 100, 1000$, and 10000, confirming boundedness of $\mathrm{E}|v(t,x)|^2$ in $x = .1$. It seems to converge even very fast with increasing number of Galerkin-Modes.
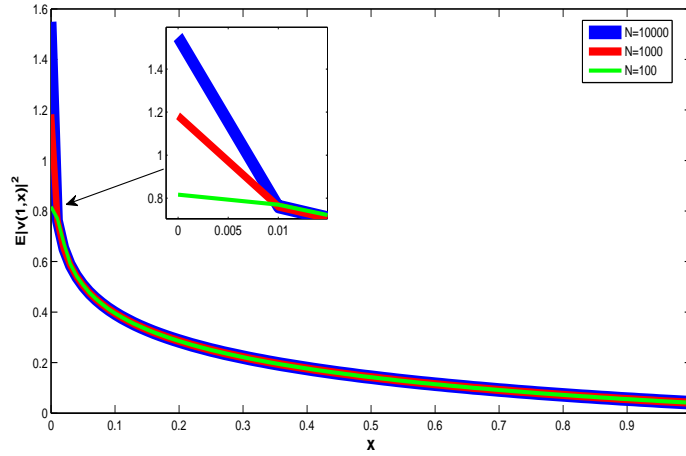

Figure 10: Approximation of $\mathrm{E}|v(t,x)|^2$ with respect to space and $t = 1$, sum of first N terms of right-hand of (14) for $N = 100, 1000$, and 10000, confirming unboundedness of $\mathrm{E}|v(t,x)|^2$ for $x = 0$ and its boundedness for $x \neq 0$.

In fact $Z(t)$ is nothing other than the mild solution of:

$$\begin{cases} \partial_t \mathbf{z} = \partial_{xx}\mathbf{z} - \alpha\partial_t\mathrm{W}, \\ \partial_x\mathbf{z}(.,0) = 0 \qquad \partial_x\mathbf{z}(.,1) = 0. \end{cases} \tag{17}$$

Note that the difference between $Z(t)$ in (16) and $v(t)$ in (4) is that the Brownian motions used in $v(t)$ are actually the same, but in $\mathrm{W}(t)$ independent Brownian motions are used. Since properties of $Z(t)$ are known to us, we try to introduce the following criteria to find relation between $Z(t)$ and $v(t)$. This is just the
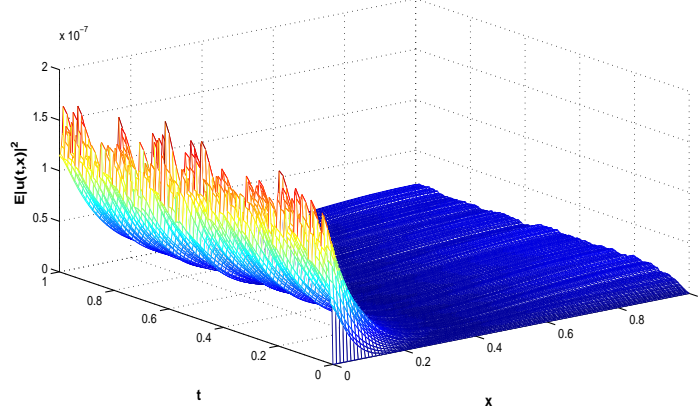
Figure 11: Approximation of $E|u(t,x)|^2$ for Burgers equation with respect to time and space, for $N = 100$.

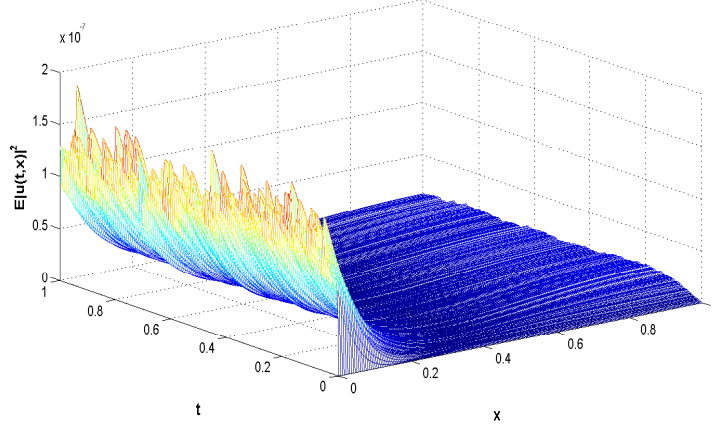

Figure 12: Approximation of $E|u(t,x)|^2$ with respect to time and space, for $N = 200$. This is for $x > 0$ very similar to Figure 11 with $N = 100$, but for $x = 0$ the values are already slightly bigger. They would grow further, if we increase N more.

same approach of [6]. The first criterion that we use is the mean energy M_u defined as:

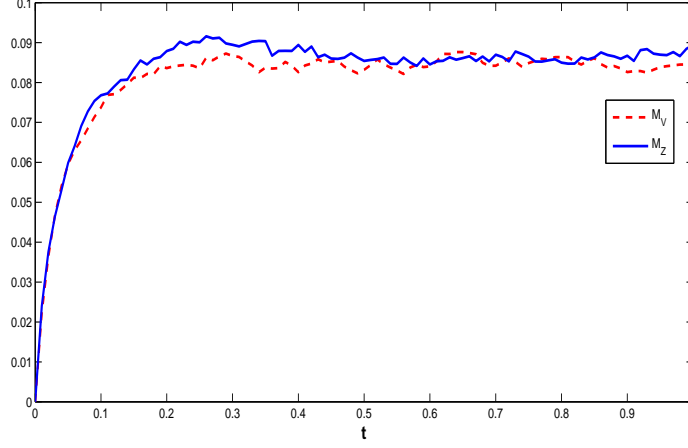$$M_u = \int_0^1 E[u(t,x) - \bar{u}(t)]^2 dx \qquad (18)$$

18

Figure 13: Numerical estimate of the mean energy M_v and M_Z to illustrate the results of Theorem 5.1. Already very few realizations in the Monte-Carlo simulation yields very good agreement of the curves.

where

$$\bar{u}(t) = \int_0^1 u(t,x)dx.$$

The second quantity is the averaged mean correlation function $\hat{C}$ defined as:

$$\hat{C}(t,r) = \frac{1}{2}\left[C(t,r) + C(t,-r)\right] \tag{19}$$

where

$$C(t,r) = \int_0^1 \mathrm{E}\left[u(t,x) - \bar{u}(t)\right]\left[u(t,x+r) - \bar{u}(t)\right]dx. \tag{20}$$

Note that $C(t,r)$ can be defined for any $r \in \mathbb{R}$ by $2l$-periodic extension. For the above mentioned criteria we can state the following Theorem.

Theorem 5.1. *Suppose $\alpha = \sigma g_1(0)$ then we have*

$$M_v = M_Z.$$

Before proving the theorem, we calculate M_v and M_Z numerically (by setting the nonlinear term 0 in (1) and $u_0 = 0$) and plot them in Figure 13, the performance confirms the result of Theorem 5.1. Even under discretization and using not that many realizations, the estimated curves for the mean values agree well.

Proof. First due to $\bar{v}(t) = \sigma g_0^2(0)\beta(t)$ we obtain

$$v(t,x) - \bar{v}(t) = \sigma g_1(0) \sum_{k=1}^{\infty} \int_0^t e^{-(t-s)\lambda_k} d\beta(s) g_k(x) . \tag{21}$$
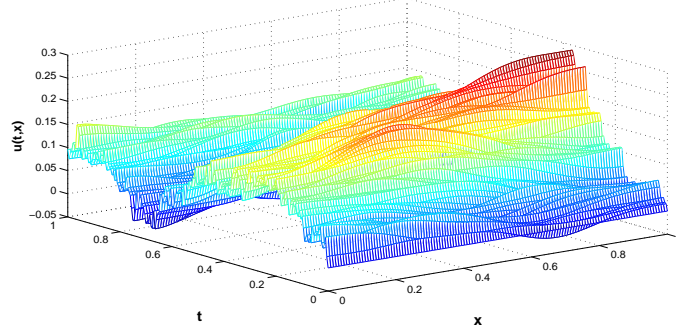
19

Figure 14: Solution of Burgers equation (27), for noise intensities $\sigma = 0.5$ and with $u_0(x)$=0 , $N = 128$. Although mean quantities agree, this is very different from boundary forcing. See Figure 15.

We have

$$M_v = \mathrm{E} \int_0^1 [v(t,x) - \bar{v}(t)]^2 dx = \mathrm{E} \int_0^1 \left(\sigma g_1(0) \sum_{k=1}^\infty \int_0^1 e^{-(t-s)\lambda_k} d\beta(s) g_k(x) \right)^2 dx \ . \tag{22}$$

Therefore, using $\int_0^1 g_k(x) g_l(x) dx = 0$ for $k \neq l$ and Itô isometry, we obtain:

$$M_v = \sigma^2 g_1^2(0) \sum_{k=1}^\infty \int_0^t e^{-2s\lambda_k} ds. \tag{23}$$

Similarly we have

$$M_{\mathrm{Z}} = \mathrm{E} \int_0^1 \left(\alpha \sum_{k=1}^\infty \int_0^1 e^{-(t-s)\lambda_k} d\beta_k(s) g_k(x) \right)^2 dx = \alpha^2 \sum_{k=1}^\infty \int_0^t e^{-2s\lambda_k} ds. \tag{24}$$

Therefore, from (23) and (24) we obtain the claim of the theorem. $\qquad \square$

According to the Theorem above, we see that they have a different structure but have the same mean energy. Nevertheless single trajectories will behave quite differently.

In the following theorem, we show that the averaged mean correlation of $v(t)$ and $Z(t)$ is also the same.

Theorem 5.2. *Suppose* $\alpha = \sigma g_1(0)$ *then*

$$\hat{C}_v(t,r) = \hat{C}_Z(t,r) \ .$$

Proof. First note that

$$g_k(x) g_m(x+r) = g_k(0) g_m(0) \cos(\pi k x) \cos(\pi m(x+r))$$
$$= \frac{1}{2} g_k(0) g_m(0) (\cos(\pi(k-m)x - \pi m r) + \cos(\pi(k+m)x + \pi m r)) \ .$$
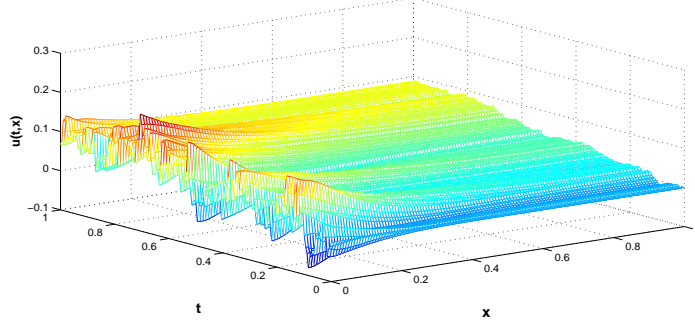
20

Figure 15: Solution of Burgers equation (1) with Neumann boundary noise, for noise intensities $\sigma = 0.5$, with $u_0(x) = 0$, and $N = 128$.

Thus using for $\ell \neq 0$ we have $\int_0^1 \cos(\pi\ell x + b)dx = \int_0^1 \cos(\pi\ell x)dx$ due to periodicity, we obtain

$$\int_0^1 g_k(x)g_m(x+r) = \begin{cases} 0 & : \quad k \neq m \ , \\ g_k^2(0)\cos(\pi r k) & : \quad k = m \ . \end{cases}$$

Hence from (21) using Itô-isometry

$$\begin{aligned} C_v(t,r) &= \int_0^1 \mathrm{E}\left[v(t,x) - \bar{v}(t)\right]\left[v(t,x+r) - \bar{v}(t)\right]dx \\ &= \sigma^2 g_1^2(0)\sum_{k=1}^{\infty}\int_0^t e^{-2(t-s)\lambda_k}ds\, g_k^2(0)\cos(\pi r k) \ . \end{aligned} \tag{25}$$

On the other hand, similarly as above, we obtain

$$\begin{aligned} C_Z(t,r) &= \int_0^1 \mathrm{E}\left[Z(t,x) - \bar{Z}(t)\right]\left[Z(t,x+r) - \bar{Z}(t)\right]dx \\ &= \alpha^2\sum_{k=1}^{\infty}\int_0^t e^{-2(t-s)\lambda_k}ds\, g_k^2(0)\cos(\pi r k). \end{aligned} \tag{26}$$

From (25) and (26) the claim follows. $\qquad\square$

We conclude from Theorems 5.1 and 5.2 that the mean energy and averaged mean correlation function for $v(\mathrm{t})$ and $Z(\mathrm{t})$ are the same while they have pathwise completely different behavior. Note that these two parameters are important tools in applied science, which are usually used in order to obtain more information about the stochastic function $v(\mathrm{t})$.

Now to compare the impact of boundary noise and body forcing noise in the
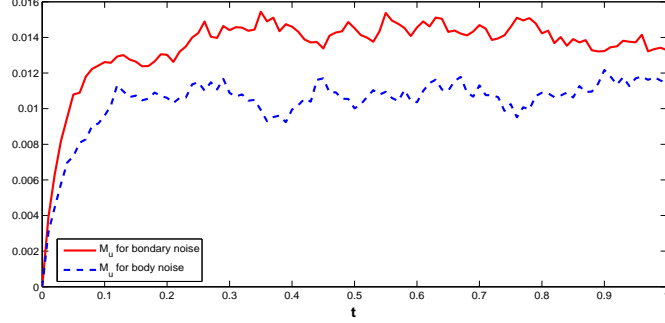
21

Figure 16: M_u for the Burgers equation (27) with body noise and the Burgers equation (1) with random Neumann boundary noise, with respect to time, for $\sigma = 0.5$, $u_0(x) = 0$, and $N = 128$.

Burgers equation we also consider

$$\begin{cases} u_t = u_{xx} - uu_x + W_t, \\ u_x(0,t) = 0 \qquad u_x(l,t) = 0, \\ u(x,0) = u_0(x). \end{cases} \qquad (27)$$

Here W_t is a Q-Wiener process with a continuous operator. We plot examples of numerical solutions of (27) and (1) in Figures 14 and 15. It is obvious that the body noise and boundary forcing noise perform completely different.

In addition we also plot M_u for (1) and (27) numerically. From Figure 16 it is seen that M_u in both cases performs similarly.

5.1. Numerical Experiments for the Rate of Convergence

In this part, we consider the pathwise approximation error of the stochastic Burgers equation with Neumann boundary noise by the method given in (10) in L^2. Note that for comparing the solutions with different N pathwise, we first calculate the noise for some large N and then use them for all smaller N. Figure 17 illustrates that, the order of convergence is $\frac{1}{2}$. Obviously these are only four examples, but all of a few hundred calculated examples behave similarly. Note that for the unknown solution, we use a numerical approximation with N sufficiently large. The Matlab code is presented for obtaining one path simulation of the method (10). Note that here A is the Laplacian with Neumann boundary conditions and thus its eigenpairs are given by

$$g_k(x) = \sqrt{\frac{2}{l}} \cos\left(\frac{\pi k x}{l}\right) \qquad \text{and} \qquad \lambda_k = -\left(\frac{k\pi}{l}\right)^2 \quad \text{for } x \in (0,1), \ \ k \in \mathbb{N}_0.$$
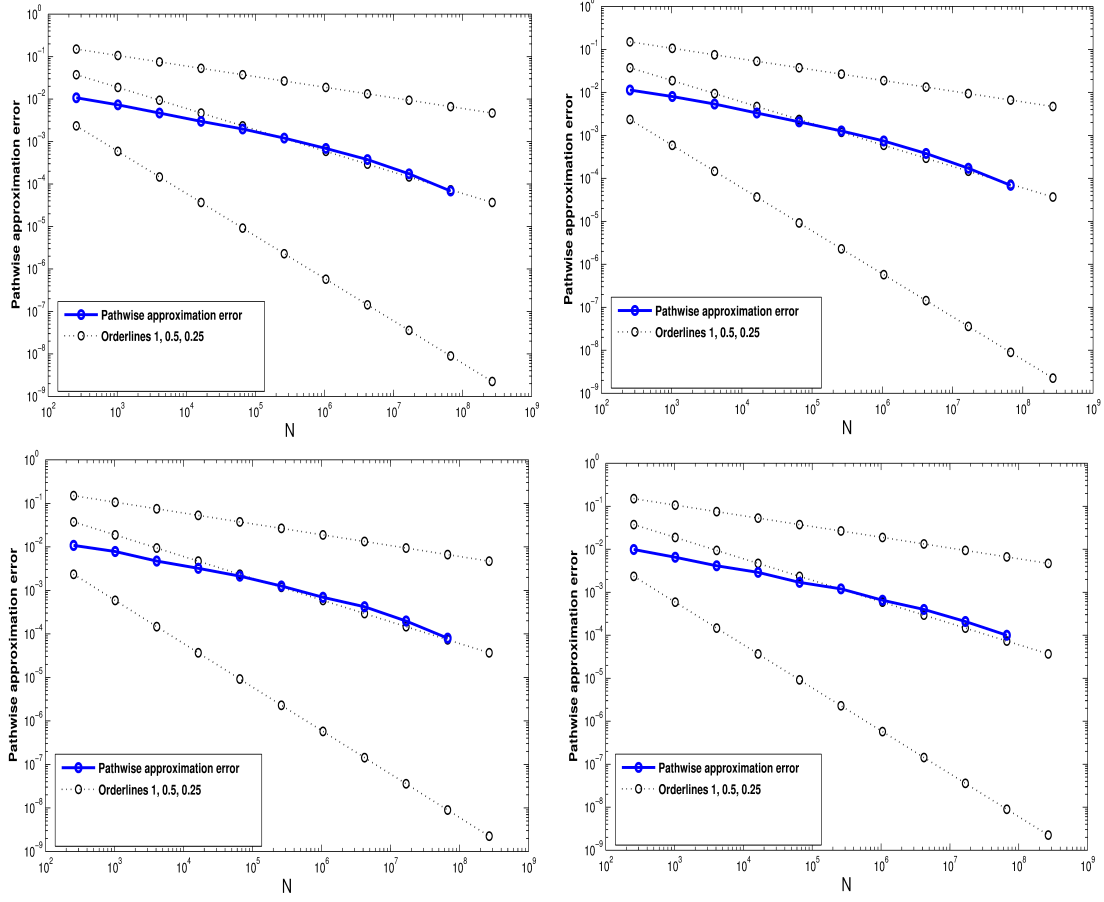
For each Fourier mode, we obtain

22

Figure 17: Pathwise approximation error against N for $N \in \{16, 32, ..., 8192\}$ for four random $\omega \in \Omega$. These are only four examples, but all other calculated trajectories behave similarly.

$$(u_{n,k+1}, g_j)_H = e^{\lambda_j} (u^N, g_j)_H = \sqrt{2} e^{\lambda_j} \int_0^1 u^N(x) \cos(j\pi x) dx \qquad (28)$$

for $k = 1, ..., N{-}1$ and therefore we use some numerical integration method (here we choose composite trapezoidal formula) to approximate $(u^N, g_j)_H$. Since the eigenfunctions $g_j(x) = \sqrt{2}\cos(j\pi x)$ are cosine functions, we can invoke built-in functions **fft** in Matlab to perform efficient computations. For this, we defined **dcts** for discrete cosine transform via **fft** in Matlab and **idctc** for composite trapezoidal formula to calculate inner products and **Ddct** to calculate F in (10).

5.1.1. Matlab code for one path simulation

function onepathsimul()

```matlab
clear all;clc;
N = 10; M = 100; SqrM = sqrt(M);
A = -pi^2*(1:N-1).^2; B = [1/M (1-exp(A/M))./A];
C = [1/SqrM sqrt((1-exp(2*A/M))./(-2*A))];
Y = [0, sqrt(2)/2, zeros(1,N-2)];
for m = 1:M
  for i=1:N
    for j=1:N
      CM(i,j)=coo(i,j);
    end
  end
  CM=chol(CM);
  y = dct_c(Y)*sqrt(2);
  Dy = -sqrt(2)*pi*Ddst([0:N-1].*Y);
  Fy = -1*y.*Dy;
  noise=1*C.*(CM'*randn(N,1))';
  Y=exp([0 A]/M).*Y+B.*idctc(Fy)*sqrt(2)+noise;
end
plot((0:N-1)/(N-1),dctc(Y)*sqrt(2));

function Z = dctc(z)
  n=length(z);
  D=zeros(2*n-2);
  D(1:n) = z;
  DD=fft(D);
  Z = real(DD(1:n));
end

function z = idctc(Z)
  n=length(Z);
  if n>2;
    Z(2:n-1) = 2*Z(2:n-1);
  end
  DD=dctc(Z)/(2*(n-1));
  z = real(DD(1:n));
end

function DF = Ddst(xx)
  n=length(xx);
  D=zeros(2*n-2);
  D(1:n) = xx;
  DD=fft(D);
  DF = -imag(DD(1:n));
end

function co=coo(i,j)
```

```
    li =(i∗**pi**)ˆ2;
    lj =(j∗**pi**)ˆ2;
    dlt =.01;
    co=(1−**exp**(−dlt ∗( li+lj )))/( li+lj );
end

end
```

6. Conclusion

We considered the Burgers equation on the interval with boundary Neumann noise on one side, and we obtained series expansion of the stochastic convolution in which each term has the same Brownian motion. Then, a combined application of the Galerkin method and the exponential Euler method is applied to solve numerically the problem through its mild solution. We showed that the noise on the boundary grows immediately to the entire domain. Also one can see that as σ is increased, the noise impact on the entire domain is also increased. Then we analyzed and illustrated some properties of the stochastic term and calculated $\mathrm{E}|v(t,x)|^2$ in order to show that $v(t,0)$ is unbounded. Then to learn more about the properties of the stochastic function $v(t)$, in the lines of [6], we also studied mean energy and mean correlation, which we then compare to a stochastic convolution arising from additive noise given by a suitable Wiener process $W(t)$ driving the SPDE in (17). Finally, we illustrate numerically that the order of convergence is $\frac{1}{2}$, see Figure 17.

[1] A. Alabert, I. Gyöngy, On numerical approximation of stochastic Burgers' equation, From stochastic calculus to mathematical finance, Springer, Berlin, (2006), 1–15.

[2] S. Peszat, J. Zabczyk, Stochastic Partial Differential Equations with Lévy Noise, Cambridge University Press, Cambridge, U.K., (2007), 241–249.

[3] E. Hausenblas, Numerical analysis of semilinear stochastic evolution equations in Banach spaces, *J. Comput. Appl. Math.*, 147 (2002), 485–516.

[4] G. Da Prato, J. Zabczyk, Ergodicity for infinite-dimensional systems, vol. 229 of London Mathematical Society Lecture Note Series. Cambridge University Press, Cambridge, 1996.

[5] I. Gyöngy, D. Nualart, On the stochastic Burgers equation in the real line, Ann. Probab. 27, 2 (1999), 782–802.

[6] D. Blömker, J. Duan, Predictability of the Burgers dynamics under model uncertainty. pp. 71–90 in Stochastic differential equations: Theory and applications. A Volume in Honor of Professor Boris L Rozovskii (Ed. P. Baxendale, S. Lototsky), 2007.

[7] A. Jentzen and P.E. Kloeden, Overcoming the order barrier in the numerical approximation of stochastic partial differential equations with additive space-time noise, *Proc. Roy. Soc. London Ser A.*, 465 (2009), 649–667.

[8] A. Jentzen, P.E. Kloeden, and G. Winkel, Efficient simulation of non-linear parabolic SPDEs with additive noise, *Ann. Appl. Probab.*, 21 (2011), 908–950.

[9] A. Jentzen, Taylor Expansions for Stochastic Partial Differential Equations. Johann Wolfgang Goethe-University, Frankfurt am Main, Germany, 2009. Dissertation.

[10] R. Sowers, Multidimensional reaction–diffusion equations with white noise boundary perturbations, Ann. Probab. 22 (1994), 2071–2121.

[11] A. Debussches, J. Printems, Numerical simulation of the stochastic Korteweg-de Vries equation, Physica D 134(2) (1999), 200–226.

[12] Z. Brzezniak, S. Peszat, Hyperbolic equations with random boundary conditions, Interdisciplinary Math. Sci. 8 (2009), 1–21.

[13] I. Gyöngy, A. Millet, Rate of convergence of space time approximations for stochastic evolution equations, Potent. Anal. 30 (2008), 29–64..

[14] C. Prevot, M. Röckner, A concise course on stochastic partial differential equations, vol. 1905 of Lecture Notes in Mathematics, *Springer, Berlin.*, 2007.

[15] J. B. Walsh, On numerical solutions of the stochastic wave equation, *Illinois J. Math.*, 50,1-4 (2006), 991–1018.

[16] T. Shardlow, Numerical methods for stochastic parabolic PDEs, *Numer. Funct. Anal. Optim.*, 20, 1-2 (1999), 121–145.

[17] I. Gyöngy, N. Krylov, An accelerated splitting-up method for parabolic equations, *SIAM J. Math. Anal.*, 37, 4 (2005), 1070–1097.

[18] I. Gyöngy, T. Martinez, On numerical solution of stochastic partial differential equations of elliptic type, *Stochastics.*, 78, 4 (2006), 213–231.

[19] T. Runst, and W. Sickel, sobolev spaces of fractional order, Nemytskij operators, nonlinear partial differential equations, vol. 3 of de Gruyter Series in Nonlinear Analysis and Applications , *Walter de Gruyter Co. Berlin.*,(1996).

[20] A. V. Balakrishnan, Identification and stochastic control of a class of distributed systems with boundary noise. Control theory, numerical methods and computer systems modelling (Internat. Sympos., IRIA LABORIA, Rocquencourt, 1974), pp. 163–178, Lecture Notes in Econom. and Math. Systems, Vol. 107, Springer, Berlin,1975. , *Walter de Gruyter Co. Berlin.*,(1996).

[21] A. Pazy, Semigroups of Linear Operators and Applications to Partial Differential Equations, *Springer*, (1992)

[22] X. Shengqiang, J. Duan, A Taylor expansion approach for solving partial differential equations with random Neumann boundary conditions. , *Applied Mathematics and Computation*, 217 (2011), 95329542.

[23] D. Blömker, M. Kamrani, S.M. Hosseini, Full discretization of the stochastic Burgers equation with correlated noise , *IMA Journal of Numerical Analysis*, (2013), 1–24.

[24] D. Henry, Geometric Theory of Semilinear Parabolic Equations Lecture Notes in Mathematics, Volume 840, (1981)